Reprinted from

journal of nuclear materials

Journal of Nuclear Materials 232 (1996) 152–158

Precipitate morphologies predicted using discrete lattice descriptions

A. Sarce *

Departamento Materiales, Centro Atómico Constituyentes, Comisión Nacional de Energía Atómica, Avda. del Libertador 8250, 1429 Buenos Aires, Argentina

Received 24 January 1996; accepted 31 May 1996

N·H

ELSEVIER

JOURNAL OF NUCLEAR MATERIALS

Scope

The Journal of Nuclear Materials publishes high quality papers in materials research relevant to nuclear fission and fusion reactor technologies, and in closely related aspects of materials science and engineering. Both original research and critical review papers covering experimental, theoretical, and computational aspects of either fundamental or applied nature are welcome. The breadth of the field is such that a wide range of processes and properties is of interest to the readership, spanning atomic lattice defects, microstructures, thermodynamics, corrosion, and mechanical and physical properties, for example. The following list, which is not exhaustive, describes topics appropriate to the Journal.

- Fission reactor materials, including fuels, cladding, core structures, pressure vessels, moderator and control components; fission product behavior.
- Materials aspects of the fabrication and reprocessing of fuels.
- Performance of nuclear waste materials, glasses and ceramics, immobilization of wastes.
- Fusion reactor materials, including first walls, blankets, insulators, and magnets.
- Neutron radiation effects in materials, including defects, microstructures, transmutations, phase changes, and macroscopic properties.
- Interactions of plasmas, ion beams, electron beams and electromagnetic radiation with materials.

Abstracted/indexed in:

Aluminium Industry Abstracts, Chemical Abstracts, Current Contents: Engineering, Computing and Technology, Current Contents: Physical, Chemical and Earth Sciences, EI Compendex Plus, Engineered Materials Abstracts, Engineering Index, INSPEC, Metals Abstracts, Physics Briefs.

Subscription Information 1996

Volumes 228–239 of Journal of Nuclear Materials (ISSN 0022-3115) are scheduled for publication. Prices are available from the publishers upon request. Subscriptions are accepted on a prepaid basis only. Issues are sent by SAL (Surface Air Lifted) mail wherever this service is available. Airmail rates are available upon request. Please address all enquiries regarding orders and subscriptions to:

Elsevier Science BV
Order Fulfilment Department
PO Box 211, 1000 AE Amsterdam
The Netherlands
Tel.: +31-20 485 3642; Fax: +31-20 485 3598.

Claims for issues not received should be made within six months of our publication (mailing) date. If not, they cannot be honoured free of charge.

US mailing notice – Journal of Nuclear Materials (ISSN 0022-3115) is published monthly, except semimonthly in April, June, September, October, November and December, by Elsevier Science BV, Molenwerf 1, PO Box 211, 1000 AE Amsterdam, The Netherlands. The annual subscription price in the USA is US$ 4215 (valid in North, Central and South America only), including air speed delivery. Second class postage paid at Jamaica, NY 11431.

USA Postmasters: Send changes to Journal of Nuclear Materials, Publications Expediting, Inc., 200 Meacham Avenue, Elmont, NY 11003. Airfreight and mailing in the USA by Publications Expediting.

♾ The paper used in this publication meets the requirements of ANSI/NISO Z39.48-1992 (Permanence of Paper).

Printed in The Netherlands

North-Holland, an imprint of Elsevier Science

ELSEVIER

Journal of Nuclear Materials 232 (1996) 152–158

journal of nuclear materials

Precipitate morphologies predicted using discrete lattice descriptions

A. Sarce *

Departamento Materiales, Centro Atómico Constituyentes, Comisión Nacional de Energía Atómica, Avda. del Libertador 8250, 1429 Buenos Aires, Argentina

Received 24 January 1996; accepted 31 May 1996

Abstract

The morphology analysis of β-85 wt% Nb precipitates in a hcp α-Zr (1 wt% Nb) matrix is performed here. The anisotropy of the diffusion of vacancies and interstitials in the matrix, as predicted by a many-body potential (EAM-type), is explicitly included in the calculations. A variable anisotropic shape of stable precipitates is predicted. This result is compared with the previous one obtained by using a short-range pair potential.

1. Introduction

In materials under irradiation, equal numbers of vacancies and self-interstitials are produced outside thermal equilibrium. These point defects migrate by thermal activation in the lattice and they may be trapped by other defects like dislocations [1], grain boundaries [2] and interfaces of precipitates [3,4]. In alloys, these point defects may have a direct effect on stability and growth of precipitate phases [5]. Maydet and Russell [6] have developed a theory which describes the behavior of incoherent intragranular spherical precipitate particles during irradiation. In the previous paper [7], Maydet and Russell's theory was modified in order to analyze the stability and morphology of the initially cubic in shape bcc β-85 wt% Nb particles in an anisotropic hcp α-Zr (1 wt% Nb) matrix under irradiation. In that work [7], the static and dynamic properties of point defects in the matrix were calculated by a short-range pair potential [8] within a discrete lattice description. An anisotropic shape of precipitates was predicted above 500 K, with the smaller dimension in the c-hexagonal crystal direction. This predicted anisotropic shape was a direct consequence of including explicitly the anisotropy of the diffusion of vacancies and interstitials, predicted using the mentioned potential, in the calculations.

Also, the stability of the same precipitates was studied in Ref. [9], where the atomic interactions of point defects in the matrix were represented by a many-body potential based on the embedded atom method (EAM) [10]. This EAM-type potential includes up to the third-neighbor shell and fits the experimental data as follows: cohesive energy exactly, vacancy formation energy and c/a ratio within 2%, elastic constants within 20%. As indicated in Section 2, it predicts equilibrium and saddle point configurations and vacancy and interstitial migration anisotropies different from those predicted using the pair potential [8].

In the present work, the values for the diffusivity tensor components on the basal plane D_a and along the c-direction D_c for vacancies and interstitials predicted by the mentioned EAM potential, are considered to analyze the evolution of the morphology of the β-85 wt% Nb stable precipitates. These precipitates are considered to be incoherent with the matrix, i.e., they can be considered as ideal sinks for point defect [4], and initially cubic in shape. As in Ref. [7], this initially cubic shape was assumed to take into account the strong dependence of the trapping at precipitates of the vacancies and interstitials on the lattice anisotropy. The modified Maydet and Russell's theory (Section 3) is used and the calculation scheme detailed in Ref. [7] is followed. The results obtained using the EAM potential (Sections 4 and 5) are compared, in Section 6, with those of the pair potential [7].

The 'rate theory' approach [3,11,12] is taken to associate the micro and macro evolution of the crystal under irradiation.

* Tel.: +54-1 754 7279; fax: +54-1 754 7404; e-mail: maestria@cnea.edu.ar.

PII S0022-3115(96)00403-5

2. Anisotropy of point defect diffusion

The dependence of the defect diffusivity with temperature for the stress free α-Zr, modeled with EAM potential [10], was determined in Ref. [13]. The interstitial jumps considered were: B_c–B_s–B_c; O–C–O and O–B_o–O (C and B_c, the crowdion configurations corresponding to an interstitial located between two nearest neighbors from adjacent basal planes (C) or from the same basal plane (B_c); O, the octahedral configuration; B_s, the split dumbell configurations corresponding to the basal plane; B_o, basal plane configuration with the interstitial directly located below the O sites (see Appendix A)). In the temperature range analyzed in that work, 300 to 800 K, both defects tend to diffuse more isotropically as temperature increases (see Table 2). For temperatures up to 520 K, the ratio (D_c/D_a) is greater for vacancies than for interstitials. From 520 K on, the reverse is true. This reversal in behavior of (D_c/D_a) for vacancies and interstitials is not obtained with the pair potential, where $(D_c/D_a)_v > (D_c/D_a)_i$ for varying temperature [14].

3. Precipitation model

As mentioned in the Introduction, Maydet and Russell [6] developed a theory which describes the behavior of incoherent intragranular precipitate particles during irradiation. Precipitates are assumed to be spherical and the matrix and precipitate are considered as binary substitutional solutions, dilute in solute and in solvent, respectively. The precipitate is characterized by two variables: x and n. The former is the number of solute atoms within the precipitate and the latter is the number of excess vacancies in it, so that $n + x$ is equal to the number of matrix atoms displaced. The rate of change in x or n, that moves the particle in the x or n directions, can be written as

$$\dot{x} = \beta_x(n, x) - \alpha_x(n, x), \tag{1}$$

$$\dot{n} = \beta_v(n, x) - \alpha_v(n, x) - \beta_i(n, x), \tag{2}$$

where β_x, β_v and β_i are the arrival rates of solutes, vacancies (v) and interstitials (i) to the precipitate and α_x and α_v are the rates of solute loss and vacancies respectively. If α_x and α_v are replaced in Eqs. (1) and (2) by their expressions as calculated in Ref. [6], nodal lines can be obtained by setting Eqs. (1) and (2) individually equal to zero. If the nodal lines intersect at n^* and x^*, the intersection point is known as the critical point. To this critical point corresponds the critical radius of the particle:

$$r^* = -2\gamma\Omega/\Delta\Phi, \tag{3}$$

where $\Delta\Phi$ is an irradiation-modified potential [15] given by

$$\Delta\Phi = -kT\left\{\ln S_x\left[S_v(1 - \beta_i/\beta_v)\right]^{\delta} + (1/4B) \times \left[\ln S_v(1 - \beta_i/\beta_v)\right]^2\right\}. \tag{4}$$

Table 1
Material and irradiation parameters

Parameter	Value	Ref.
K (displacement rate)	1.4×10^{-7} dpa/s	assumed
a_{Zr} (lattice parameter α-Zr)	0.323 nm	[24]
a_{pr} (parameter of β-85wt%Nb)	0.335 nm	[24]
Ω_m (atomic volume of matrix)	23.26×10^{-3} nm^3	calculated
Ω (atomic volume of β phase)	18.10×10^{-3} nm^3	calculated
T (temperature)	K	assumed
T_m (Zr melting point)	2128 K	[22]
k (Boltzmann's constant)	0.862×10^{-4} eV/K	
E (Young's modulus for α-Zr at 573 K)		
100 direction	466 eV/nm^3	[25]
001 direction	613 eV/nm^3	[25]
ν (Poisson's ratio for α-Zr at 573 K)		
100 direction	0.37	[25]
001 direction	0.48	[25]
γ (particle:matrix energy)	3.12×10^{-4} eV/nm^2	assumed
D_0 (diffusivity pre-exponent for the vacancy in α-Zr)	4.6×10^{-6} m^2/s	[10]
E_v^f (vacancy formation energy)	1.36 eV	[10]
c_v^e (equilibrium vacancy concentration in α-Zr)	$\exp(-E_v^f/kT)$	calculated
c_x^e (solubility of Nb in α-Zr)	0.6 wt%	[22]
c_x (concentration of Nb in the α-Zr matrix)	1 wt%	assumed
$S_x = c_x/c_x^e$ (impurity atom supersaturation)	1.67	calculated

In this expression, S_v is the vacancy supersaturation in the irradiated matrix defined as

$$S_v = c_v/c_v^e, \tag{5}$$

c_v^e being the thermal equilibrium vacancy concentration and c_v the actual vacancy concentration in the matrix.

$$\delta = (\Omega - \Omega_m)/\Omega_m \tag{6}$$

and

$$B = \Omega E/9kT(1-\nu). \tag{7}$$

The meaning and values of other symbols are summarized in Table 1.

Precipitates with $r > r^*$ will grow, while if they have $r < r^*$, they will decay.

Unlike Maydet and Russell's theory, initially cubic precipitates in an hexagonal matrix, are assumed in this work. From the anisotropy of the diffusion tensor in hcp lattice, each face in the precipitate takes up a different number of vacancies and a different number of interstitials, according to its orientation with respect to the crystal lattice. Then, (β_i/β_v) and $\Delta\Phi$ values are distinct for different faces. Consequently, there is a critical size in each j geometrical direction parallel to the edge of precipitate. Each critical size, the smallest size d_j^* that a particle under irradiation must have in a j direction in order to grow in this direction (critical size in the j direction) results, in the modified Maydet and Russell's theory [7]:

$$d_j^* = -3.2\gamma\Omega/\Delta\Phi_j, \tag{8}$$

where

$$\Delta\Phi_j = -kT\left\{\ln S_v\left[S_v(1-\beta_{ij}/\beta_{vj})\right]^{\delta} + (1/4B) \times \left[\ln S_v(1-\beta_{ij}/\beta_{vj})\right]^2\right\}, \tag{9}$$

β_{ij} (β_{vj}) being the arrival rate of interstitials (vacancies) to the precipitate face perpendicular to the j direction, assuming the interphase precipitate-matrix to be incoherent.

In general, precipitate with $d_j > d_j^*$ will grow, while if they have $d_j < d_j^*$ or $\Delta\Phi_j > 0$, they are unstable and will decay in the j direction [6,7].

4. Parameter evaluation

To analyze the morphology evolution of the initially cubic precipitates, the values of d_j^* for different conditions must be calculated. Therefore, all parameters in $\Delta\Phi_j$ must be evaluated.

4.1. Vacancy supersaturation

By assuming an effective productive rate of free vacancies and interstitials K, for the steady state case, c_v is [16]

$$c_v = \left(k_i^2\langle D_i\rangle/2\alpha\right)\left\{-1+\mu+\left[(1+\mu)^2+\xi\right]^{1/2}\right\}, \tag{10}$$

where

$$\mu = \alpha c_v^e/k_i^2\langle D_i\rangle \tag{11}$$

and

$$\xi = 4\alpha K/\left(k_v^2\langle D_v\rangle k_i^2\langle D_i\rangle\right). \tag{12}$$

$\langle D_v\rangle$ and $\langle D_i\rangle$ are the average vacancies and interstitials diffusivities. $\langle D_v\rangle$ is taken as [17]

$$\langle D_v\rangle = \left[D_1D_2D_3\right]^{1/3}, \tag{13}$$

where D_n, $n = 1, 2, 3$, are the eigenvalues of the diffusivity tensor in the crystal coordinate axes, calculated using the EAM potential [10]. α is the mutual interstitial–vacancy recombination constant. Kidson [18] performed a thorough investigation on how to calculate this coefficient, with a particular application to Zr. In that work he concludes that the value of

$$\alpha = 21\langle D_i\rangle/a_{Zr}^2 \tag{14}$$

obtained by Fainstein-Pedraza et al. [19] is about right in that they obtain good agreement with the measured irradiation growth. Therefore, the value given by Fainstein-Pedraza et al. is taken in this work. k_v^2 and k_i^2 are the total sink strengths for vacancies and interstitials considering all sinks present in the irradiated material (i.e., dislocations, grain boundaries and precipitates). These sink strengths, calculated within the 'rate theory' formulation, can be approximated by polynomials in (D_c/D_a) [7,13,20] (see Appendix B). Then, c_v can be obtained.

4.2. (β_{ij}/β_{cj}) ratio

From Section 3, the behavior of different precipitate faces will be taken into account explicitly in order to calculate (β_{ij}/β_{vj}) in $\Delta\Phi_j$. Henceforth, for simplicity in the analysis of results, the c-lattice and the a-lattice axes are taken to be parallel to the edges of the precipitate.

From the definition of precipitate partial sink strengths [7], the ratio (β_{ic}/β_{vc}) for the precipitate face perpendicular to c-lattice direction can be calculated as

$$(\beta_{ic}/\beta_{vc}) = \left(k_{cpri}^2\langle D_i\rangle c_i\right)/\left(k_{cprv}^2\langle D_v\rangle c_v\right) \tag{15}$$

and the ratio (β_{ia}/β_{va}) for the faces parallel to a-lattice direction as

$$(\beta_{ia}/\beta_{va}) = \left(k_{apri}^2\langle D_i\rangle c_i\right)/\left(k_{aprv}^2\langle D_v\rangle c_v\right), \tag{16}$$

where k_{cpr}^2 is the sink strength of the precipitate face perpendicular to the c-axis and k_{apr}^2 the sink strength of the faces parallel to c-axis. $k_{cpri,v}^2$, $k_{apri,v}^2$, $\langle D_v\rangle$ and c_v can be calculated using Eqs. (B.4) (see Appendix B), (B.5) (see Appendix B), (13) and (10), respectively.

Finally, for the same conditions as 3.1 c_i, the actual interstitial concentration, is [16]

$$c_i = \left(k_v^2\langle D_v\rangle/2\alpha\right)\left\{-(1+\mu)+\left[(1+\mu)^2+\xi\right]^{1/2}\right\}. \tag{17}$$

The β_i/β_v ratio does not depend on $\langle D_i\rangle$.

5. Application to the annealed state of Zr–2.5 wt% Nb system

The Zr–2.5 wt% Nb alloy is of particular interest because it is used in the pressure tubes of CANDU reactors. Consequently, several studies were performed to investigate the behavior of the system under neutron irradiation. In particular, Coleman et al. [21] irradiated a Zr–2.5 wt% Nb alloy in the Oak Ridge reactor at different temperatures and different doses at a displacement rate of about 1.4×10^{-7} dpa/s. In the annealed state material with a microstructure of hcp α-Zr grains with bcc β-phase at the grain boundaries, irradiation in the 570–770 K range resulted in precipitation of β-Nb in the α-phase. This β-Nb phase appeared to nucleate homogeneously down to about 700 K.

The modified Maydet and Russell's theory is applied in this section to analyze this precipitation. To calculate $\Delta\Phi_j$, except for S_v, the irradiated α-Zr (1 wt% Nb) matrix is assumed to be α-Zr pure phase, and consisting of cubic grains of 2×10^{-6} m in size with a homogeneous prismatic dislocation density $\rho_d = 10^{12}$ m^{-2} and a homogeneous density of 9×10^{19} m^{-3} initially cubic precipitates of 0.03×10^{-6} m in size within them. The α-Zr pure phase is described by the mentioned EAM-type potential [10]. From the phase diagram [22], $S_v = 1.67$.

The calculated values for vacancy supersaturations S_v for different temperatures and assuming an effective productive rate equal to 1.4×10^{-7} dpa/s, and the β_i/β_v ratio calculated for different faces and temperatures, are given in Table 2. These different faces of the precipitate are considered separately, in order to calculate $\Delta\Phi_j$ and later d_j^*.

5.1. Faces perpendicular to c-lattice direction

5.1.1. 330–520 K range ($(\beta_{ic}/\beta_{vc}) < 1$)

Fig. 1 shows the d_c^*/a_{pr} values for different temperatures obtained from parameters shown in Tables 1 and 2, introduced in Eq. (9) and later in Eq. (8). B values are calculated taking $E(100)$ and $\nu = [\nu(100) + \nu(001)]/2$ because the growth in the c-direction is analyzed [7]. From $T = 500$ K on, $\Delta\Phi_c$ is positive (see Fig. 2) and the particle will decay in this direction. In Fig. 1, as a comparison, the corresponding values d_c^*/a_{pr} calculated using a pair potential (from Ref. [7]) and calculated for the case of non-irradiation (in this case $\Delta\Phi = -kT \ln S_v$ [5]) are shown. The values of r_c^* change when the effective productive rate of free vacancies and interstitials (the latter being smaller than the displacement rate in the case of the fast neutron irradiation) is changed: they increase if K decreases and decrease if K increases. This is fundamentally a consequence of the dependence of S_v on K (S_v is approximately proportional to $K^{1/2}$). However, the tendency shown in Fig. 1 is not modified.

Table 2
$(D_c/D_a)_i$, (β_i/β_v) and vacancy supersaturation (S_v)

T	$(D_c/D_a)_i$	$(D_c/D_a)_v$ [13]	β_{ic}/β_{vc} [13]	β_{ia}/β_{va}	S_v
330	0.19	0.31	0.85	1.02	8.0×10^{27}
400	0.30	0.39	0.92	1.02	1.3×10^{21}
450	0.39	0.44	0.95	1.01	3.5×10^{17}
500	0.46	0.48	0.99	1.00	5.1×10^{14}
560	0.55	0.52	1.02	0.99	9.1×10^{11}
600	0.60	0.54	1.04	0.97	2.7×10^{10}
673	0.68	0.58	1.07	0.96	1.3×10^{8}
773	0.77	0.62	1.10	0.95	4.5×10^{5}

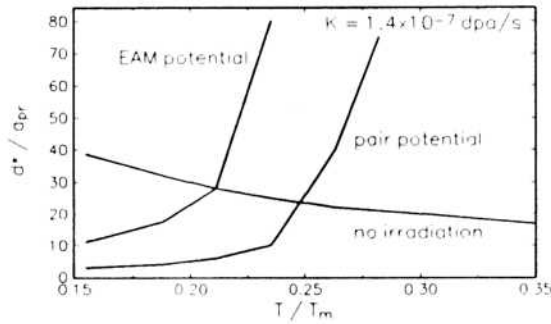

Fig. 1. Critical size d^*/a_{pr} ratio as a function of homologous temperature (T/T_m) for the precipitation of β-85 wt% Nb in the anisotropic α-Zr matrix under irradiation, $(\beta_{ic}/\beta_{vc}) < 1$ case. (a) predicted using the EAM-type potential [10]. (b) Predicted using a pair potential (from Ref. [7]). (c) Predicted for the non-irradiation case.

5.1.2. 520–773 K range ($(\beta_{ic}/\beta_{vc}) > 1$)

In this case it is not possible to calculate a priori $\Delta\Phi_c$, and consequently d_c^*. However, as it was analyzed in Ref. [7], as the interstitial sites in the bcc structure are smaller than $0.25r$, where r is in this case the Nb atomic radius,

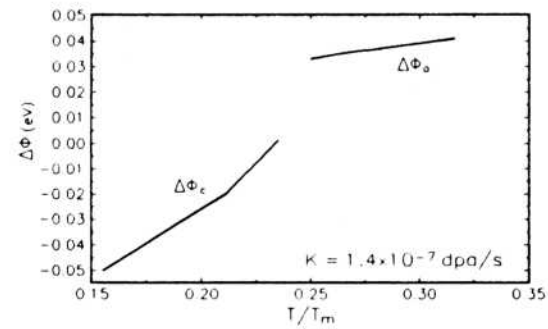

Fig. 2. Irradiation-modified potential $\Delta\Phi_c$ ($(\beta_{ic}/\beta_{vc}) < 1$ case) and irradiation-modified potential $\Delta\Phi_a$ ($(\beta_{ia}/\beta_{va}) < 1$ case) as a function of homologous temperature (T/T_m) for the precipitation of β-85 wt% Nb in the anisotropic α-Zr matrix under irradiation.

the irradiation-induced Zr self-interstitials would not occupy those sites. Then, only an equal number of vacancies and self-interstitials could jump into the precipitate. In the limit case $\beta_i = \beta_v$, Eqs. (9) and (8) predict $d_c^* = 0$. Therefore, if $T > 520$ K, all particles will be able to grow in the c-crystal direction, independent of their initial size.

5.2. Faces parallel to c-lattice direction

5.2.1. 300–520 K range ($(\beta_{ia}/\beta_{va}) > 1$)

Using the same considerations of Section 5.1.2, it can be predicted that $d_a^* = 0$. Then, up to 520 K, all particles will be able to grow in the a-crystal direction.

5.2.2. 520–773 K range ($(\beta_{ia}/\beta_{va}) < 1$)

Within this temperature range, $\Delta\Phi_a$ results positive (see Fig. 2) and the particle will not be able to grow in the a-crystal directions. This behavior is not changed, even if K is decreased or increased by two orders of magnitude. B values are calculated taking $E(001)$ and $\nu = \nu(100)$.

6. Discussion and conclusions

In this paper, critical sizes (the smallest size that an initially cubic particle must have in a particular direction in order to grow in that direction) in the a (d_a^*) and c (d_c^*) crystal directions for the growth of the bcc β-85 wt% Nb precipitates in a hcp α-Zr (1 wt% Nb) matrix, are calculated. The atomic interactions of point defects in this matrix, assumed to be α-Zr pure, are described by a many-body potential based on the embedded atom method (EAM) [10]. Within this description, for temperatures up to 520 K, the ratio (D_c/D_a) is greater for vacancies than for interstitials. From 520 K on, the reverse is true. As a consequence of this behavior, at temperatures $T \leq 520$ K, the arrival rate interstitial–vacancy ratio to the precipitate faces perpendicular to c is: $(\beta_{ic}/\beta_{vc}) < 1$ and to the precipitate faces perpendicular to a: $(\beta_{ia}/\beta_{va}) > 1$. On the contrary, from 520 K on, $(\beta_{ic}/\beta_{vc}) > 1$ and $(\beta_{ia}/\beta_{va}) < 1$. In the first case, $T \leq 520$ K, $d_a^* = 0$ and all particles will be able to grow in the a-crystal directions. In the same temperature range, the calculated d_c^* have finite values (different to zero). Also, from Fig. 1, it can be seen that, at low temperatures ($T \leq 450$ K) the formation of β-85 wt% Nb precipitates in the α-Zr (1 wt% Nb) phase is enhanced by irradiation and, as the critical sizes d_c^* are small, these precipitates will be practically cubic shaped. For $T > 500$ K, $\Delta\Phi_c$ is positive, and the particles will not be able to grow in the c-lattice direction. Then, precipitates will start to be anisotropic, with the smaller size in the c-crystal direction and in the 500–520 K range, precipitate would be aligned in layers parallel to the (0001) planes.

From 520 K on, the results are different. In fact, in this case $\Delta\Phi_a$ is positive and the particle will not be able to grow in these directions, on the contrary, $d_c^* = 0$. Then, above 520 K, a different morphology is predicted: rod shaped stable precipitates with the larger dimension coincident with the c-hexagonal crystal direction.

The first described morphology is in agreement with experimental observations [23]. Also, similar results are obtained in the 330–773 K range when a short-range pair potential is used to describe vacancy and interstitial migration anisotropies [7]. To the author's knowledge the second morphology is not experimentally observed and is also not predicted if a pair potential is used [7]. Then, for the pair potential previously used in Ref. [7], prediction of the morphology of the β-85 wt% Nb seems to agree better with the experimental tendency than the EAM-type [10] one.

The predicted variable anisotropic shape of stable precipitates β-85 wt% Nb in the Zr–1 wt% Nb matrix described by the EAM potential [10], is a consequence of the change of the anisotropy factor ratio $(D_c/D_a)_i/(D_c/D_a)_v$ near 520 K (< 1 at lower temperatures and > 1 at higher temperatures). On the contrary, the pair potential [8] predicts $(D_c/D_a)_i/(D_c/D_a)_v < 1$ in the temperature range analyzed. Consequently, a non-variable anisotropic shape is obtained using the later potential. It would be interesting to use another EAM-type potential (for example the improved version [26] of the EAM-type potential developed by Pasianot and Savino [27]) in order to analyze again the morphology of β-precipitates. In the light of the corresponding results, it would be possible to decide if the variable anisotropic shape of precipitates (as a consequence of the change of the anisotropy factor ratio), is a general prediction when EAM-type potentials are used to represent the α-Zr lattice.

The above comparisons show the strong dependence of predictions of macroscopic material behavior under irradiation on the interatomic potential, i.e., on the microstructure description. As it is well know, this is an indication of the strong dependence of macroscopic material behavior under irradiation on the crystal lattice symmetries, on the microstructural defects and on the processes involving defect interactions.

Acknowledgements

The author would like to thank Dr. E.J. Savino for his comments on the manuscript. This work was partially supported by the 'Proyecto Multinacional de Investigación y Desarrollo en Materiales' OEA-CNEA (Organization of American States-National Atomic Energy Commision of Argentina).

Appendix A

A.1. Interstitial migration paths

Fig. 3 shows the path corresponding to the unidirectional migration of the basal crowdion B_c, B_s being the

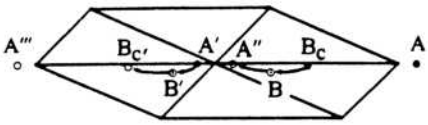

Fig. 3. Unidirectional migration path $B_s - B_s - B_c$ in the basal plane by a replacement mechanism, the basal dumbbell B_s being the saddle-point configuration. (From fig. 1 of Ref. [13].)

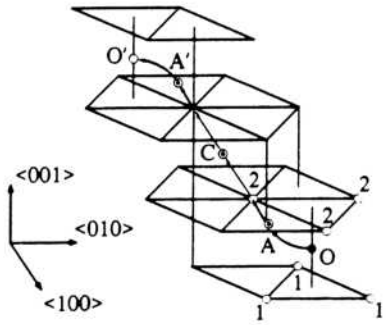

Fig. 4. Three-dimensional migration path O–C–O by a replacement mechanism, the nonbasal crowdion C being the saddle-point configuration. (From fig. 2 of Ref. [13].)

saddle point. The jump distance ($B_c \rightarrow B_{c'}$) is the basal lattice parameter a [13].

The second path considered in Section 2, O–C–O, is schematically shown in Fig. 4. It is three-dimensional and takes place by the replacement mechanism indicated in this figure [13].

The last path mentioned in Section 2, is unidirectional along the c-axis and takes place by a direct jump of the extra-atom from O to B_o, being the jump distance $c/2$ [13].

Appendix B

B.1. Sink strength calculations

Numerical calculations within the 'rate theory' formulation by Sarce and Savino [28], show that for a grain of given shape and size, and for a given effective strength k_{sc}^2 of the bulk sinks, the grain boundary sink strength depends only on the ratio (D_c/D_a) of the defect diffusivity. Also, if the precipitate size, the precipitate density and the metallurgical state of the matrix are fixed, the partial precipitate sink strengths depend only on the anisotropy factor (D_c/D_a) [7]. As in the case of the grain boundary and precipitate strengths, the whole analytic expression of the dislocation sink strength is also a function of (D_c/D_a) [14]. From figs. 2 and 3 of Ref. [14] and fig. 4 of Ref. [7], the prismatic dislocation sink strength and the grain boundary and precipitate partial sink strengths can be approximated by cubic polynomials in (D_c/D_a) [7,13,20] as

$$k_d^2 = \left[1.90 - 1.11(D_c/D_a) + 0.41(D_c/D_a)^2 - 0.05(D_c/D_a)^3\right] \times 10^{12}\ \mathrm{m}^{-2}, \quad \text{(B.1)}$$

$$k_{a\mathrm{GB}}^2 = \left[1.61 - 1.06(D_c/D_a) + 0.55(D_c/D_a)^2 - 0.10(D_c/D_a)^3\right] \times 10^{12}\ \mathrm{m}^{-2}, \quad \text{(B.2)}$$

$$k_{c\mathrm{GB}}^2 = \left[0.41 + 0.73(D_c/D_a) - 0.16(D_c/D_a)^2 + 0.02(D_c/D_a)^3\right] \times 10^{12}\ \mathrm{m}^{-2}, \quad \text{(B.3)}$$

$$k_{a\mathrm{pr}}^2 = \left[1.22 - 0.29(D_c/D_a)\right] \times 10^{13}\ \mathrm{m}^{-2}, \quad \text{(B.4)}$$

and

$$k_{c\mathrm{pr}}^2 = \left[0.41 + 0.62(D_c/D_a)\right] \times 10^{13}\ \mathrm{m}^{-2}, \quad \text{(B.5)}$$

where k_d^2 is the prismatic dislocation sink strength, $k_{c\mathrm{GB}}^2$ ($k_{c\mathrm{pr}}^2$) the sink strength of the grain boundary face (precipitate face) perpendicular to the c-axis, and $k_{a\mathrm{GB}}^2$ ($k_{a\mathrm{pr}}^2$) the sink strength of the faces parallel to c-axis. The numerical coefficients result from assuming a low dislocation density of $10^{12}\ \mathrm{m}^{-2}$ and a density of $9 \times 10^{19}\ \mathrm{m}^{-3}$ cubic precipitates of 0.03×10^{-6} m in size within cubic grains of 2×10^{-6} m in size. In particular, the dependence on (D_c/D_a) in Eqs. (B.4) and (B.5) is valid in the $(D_c/D_a) = 0.1 - (D_c/D_a) = 0.8$ range only. Finally,

$$k_{v,i}^2 = k_{\mathrm{dv},i}^2 + 2k_{a\mathrm{GBv},i}^2 + k_{c\mathrm{GBv},i}^2 + 2k_{a\mathrm{prv},i}^2 + k_{c\mathrm{prv},i}^2. \quad \text{(B.6)}$$

If $(D_c/D_a)_i$ or $(D_c/D_a)_v$ values obtained using the EAM potential [10] (Table 2) replace (D_c/D_a) in Eqs. (B.1) to (B.5), the corresponding sink strengths may be obtained for vacancies and interstitials at different temperatures.

References

[1] P.T. Heald and M.V. Speight, Acta Metall. 23 (1975) 1389.
[2] R. Bullough, M.R. Haynes and C.H. Wood, J. Nucl. Mater. 90 (1980) 44.
[3] A.D. Brailsford and R. Bullough, J. Nucl. Mater. 44 (1972) 121.
[4] A.D. Brailsford and L.K. Mansur 103–104 (1981) 1403.
[5] F.V. Nolfi, ed., Phase Transformation During Irradiation (Applied Science, London, 1983).
[6] S.I. Maydet and K.C. Russell, J. Nucl. Mater. 64 (1977) 101.
[7] A. Sarce, J. Nucl. Mater. 185 (1991) 214.
[8] A.M. Monti, Phys. Status Solidi B167 (1991) 37.
[9] A. Sarce, in: Proc. First Argentina–USA Bilateral Symp. on Materials Science and Engineering (1995), Anales de la Asociación Química Argentina (1996), accepted for publication.

[10] J.R. Fernández and A.M. Monti, Phys. Status Solidi B179 (1993) 337.
[11] H. Wiedersich, in: Physical Metallurgy of Reactor Fuel Elements, eds. J.E. Harris and E.C. Sykes (Berkeley Nuclear Laboratories, 1973) p. 142.
[12] C.H. Woo, J. Nucl. Mater. 159 (1988) 237.
[13] J.R. Fernández, A.M. Monti, A. Sarce and N. Smetniansky-De Grande, J. Nucl. Mater. 210 (1994) 282.
[14] A.M. Monti, A. Sarce, N. Smetniansky-De Grande, E.J. Savino and C.N. Tomé, Philos. Mag. A63 (1991) 925.
[15] M.R. Mruzik and K.C. Russell, J. Nucl. Mater. 78 (1978) 343.
[16] A.D. Brailsford and R. Bullough, J. Nucl. Mater. 48 (1973) 87.
[17] U.M. Gösele, Prog. React. Kinet. 13 (1984) 63.
[18] G.V. Kidson, J. Nucl. Mater. 118 (1983) 115.
[19] D. Fainstein-Pedraza, E.J. Savino and A.J. Pedraza, J. Nucl. Mater. 73 (1978) 151.
[20] A. Sarce, J. Nucl. Mater. 208 (1994) 300.
[21] C.E. Coleman, R.W. Gilbert, G.J.C. Carpenter and G.C. Weatherly, in: Phase Stability During Irradiation, eds. J.R. Holland, L.K. Mansur and D.I. Potter (TMS-AIME, Warrendale, PA, 1981) p. 587.
[22] J.P. Abriata and J.C. Bolcich, Bull. Alloy Phase Diagr. 3(1) (1982) 34.
[23] M. Griffits, J. Nucl. Mater. 159 (1988) 190.
[24] S.A. Albridge and B.A. Cheadle, J. Nucl. Mater. 42 (1972) 32.
[25] S. Terlisky, private communication.
[26] J.R. Fernández, A.M. Monti and R.C. Pasianot, Proc. Mater. Res. Soc. 318 (1994).
[27] R.C. Pasianot and E.J. Savino, Phys. Rev. B45 (1992) 12704.
[28] A. Sarce and E.J. Savino, Phys. Status Solidi B159 (1990) 557.

JOURNAL OF NUCLEAR MATERIALS

Abbreviated Instructions to Authors (see Vol. 230 (1) for the full Instructions)

Submission of papers

Manuscripts should be submitted in duplicate to one of the journal editors:

L.K. Mansur (chairman)
Metals and Ceramics Division
Oak Ridge National Laboratory
PO Box 2008
Oak Ridge, TN 37831-6376, USA
S. Ishino
Department of Nuclear Engineering
Tokai University
1117 Kitakaname, Hiratsuka-shi
Kanagawa-ken 259-12, Japan
H. Kleykamp
Forschungszentrum Karlsruhe GmbH
Institut für Materialforschung
Postfach 3640
76021 Karlsruhe, Germany
G. Saada
Laboratoire d'Etude des Microstructures
Unité Mixte CNRS-ONERA (UMR104)
BP 72
92320 Châtillon Cedex, France
L.O. Werme
Swedish Nuclear Fuel and Waste Management Co.
Box 5864
S-102 48 Stockholm, Sweden

Original material: Submission of a manuscript implies it is not being simultaneously considered for publication elsewhere and that the authors have obtained the necessary authority for publication.

Types of contributions

Original research papers and critical review papers are welcome. These may be written in English, French or German. All should contain an abstract written in English and of length less than 150 words.

Rapid publication. Short papers of total length less than 2000 words may be published as Letters to the Editors in a shorter time than regular articles as the proofs will normally be checked by the Publisher. Abstracts for Letters to the Editors should be limited to 75 words.

Manuscript preparation

The paper copies of manuscripts should be prepared with double line spacing and wide margins, on numbered sheets. See notes opposite on electronic version of manuscripts.

Structure. Please adhere to the following order of presentation: Article title, Author(s), Affiliation(s), Abstract, PACS codes and keywords, Main text, Acknowledgements, Appendices, References, Figure captions, Tables.

Corresponding author. The name, complete postal address, telephone and fax numbers and the e-mail address of the corresponding author should be given on the first page of the manuscript.

References. References to other work should be consecutively numbered in the text using square brackets and listed by number in the Refence list. Please refer to a recent issue of the journal for examples.

Figures

Figures should also be submitted in duplicate: one master set and one set of copies. The *line drawings* in the master set should be original laser printer or plotter output or drawn in black india ink, with careful lettering, large enough (3–5 mm) to remain legible after reduction for printing. The *photographs* should be originals, with somewhat more contrast than is required in the printed version. They should be unmounted unless part of a composite figure. Scale markers must be inserted on the photographs.

Colour plates. Figures may be published in colour, if this is judged essential by the editor. The publisher and the author will each bear part of the extra costs involved. Further information is available from the publisher.

Classification codes/keywords

Please supply one to four classification codes (PACS and/or MSC). See the advertisement in the final pages of this issue for further details on where to find these lists.

After acceptance

Notification. You will be notified by the Editor of the journal of the acceptance of your article and invited to supply an electronic version of the accepted text. The Editors will assign key words to manuscripts according to a subject index especially prepared for the Journal.

Copyright transfer. In the course of the production process you will be asked to transfer the copyright of the article to the publisher. This transfer will ensure the widest possible dissemination of information.

Proofs. When the page proofs of the accepted manuscript are made and sent to authors, this is in order to check that no undetected errors have arisen in the typesetting (or file conversion) process. Only printers' errors may be corrected; no changes in, or additions to, the edited manuscript will be accepted. In case of extended changes, the authors will be required to pay part of the extra costs involved.

Electronic manuscripts

The publisher welcomes the receipt of an electronic version of your accepted manuscript. Authors are requested to submit an electronic version of their manuscript to the Editor along with a paper copy. Most manuscripts require revision after refereeing; the electronic version should be included for the first time when the revised copy is submitted to the Editor. See the advertisement in the final pages of this issue for further details. Please note that no deviations from the version accepted by the Editor of the journal are permissible without the prior and explicit approval by the Editor. Such changes should be clearly indicated on an accompanying printout of the file.

Author benefits

No page charges. Publishing in Journal of Nuclear Materials is free.

Free offprints. The corresponding author will receive 50 offprints free of charge. An offprint order form will be supplied by the publisher for ordering any additional paid offprints.

Discount. Contributors to Elsevier Science journals are entitled to a 30% discount on all Elsevier Science books.

Further information (after acceptance by the Editor)

Elsevier Science BV
Journal of Nuclear Materials
Issue Management
PO Box 2759, 1000 CT Amsterdam
The Netherlands
Fax: +31-20 485 2319
E-mail: g.anderton@elsevier.nl

North-Holland, an imprint of Elsevier Science